2004

Optical absorption in terahertz-driven quantum wells

X. W. Mi
Chinese Academy of Sciences, Shanghai, China

J. C. Cao
Chinese Academy of Sciences, Shanghai, China

C. Zhang
University of Wollongong, czhang@uow.edu.au

Optical absorption in terahertz-driven quantum wells

X. W. Mi and J. C. Cao[a)]

State Key Laboratory of Functional Materials for Informatics, Shanghai Institute of Microsystem and Information Technology, Chinese Academy of Sciences, 865 Changning Road, Shanghai, 200050, People's Republic of China

C. Zhang

School of Engineering Physics and Institute of Superconducting and Electronic Materials, University of Wollongong, New South Wales 2522, Australia

The optical absorption spectra in a quantum well driven both by an intense terahertz (THz) and by an optical pulse are theoretically investigated within the theory of density matrix. We found that the optical absorption spectra and the splitting of the excitonic peaks splitting can be controlled by changing the THz field intensity and/or frequency. The Autler–Towns splitting is a result of the THz nonlinear dynamics of confined excitons, which is in agreement with the experiments. In addition, the dependence of the optical absorption on the quantum well width and the carrier density is also discussed. © *2004 American Institute of Physics.* [DOI: 10.1063/1.1635974]

I. INTRODUCTION

Modern optical telecommunications devices, such as optical switches, high-performance optical modulators,[1] and wavelength division multiplexing,[2,3] require one to understand the characteristics of optical absorption of the high-frequency radiation in semiconductors. Recently, the intense terahertz (THz)-induced optical absorption[4–8] of quantum wells (QWs) near the band gap edge has attracted considerable interest. When a QW is radiated by both an intense terahertz and an optical pulse, there are many interesting nonlinear phenomena, including ac Stark effect,[1] harmonic generation,[9] and Franz–Keldysh effect.[10,11] Many theoretical models were proposed to study these phenomena. Using the few-level model, the effects of an intersubband field on the interband and intersubband absorptions were studied.[12,13] Meanwhile, the optical absorption in semiconductors including excitonic effect are studied by using the excitonic basis and free-basis model.[1,14] Recently, the optical absorption of QWs was studied by finite-difference time-domain techniques.[3] The results show that when an external electric field is applied in the growth direction of a QW,[15] the quantum-confined Stark effect (QCSE) shows up. QCSE leads to a redshift of the absorption peak near the band gap, and generates additional absorption peaks.

The purpose of this article is to apply the density matrix theory to study the optical absorption and the coherent ultrafast dynamics of the QWs under the influence of the dc bias and the THz radiation along the QW growth direction. We present in detail the dependence of the optical absorption on the QW with and the doping concentration. It is shown that the QCSE shows up when the QW is radiated by THz field. There are multiple absorption replica in the absorption spectrum of the biased QW driven by the THz field. When

we change the THz field intensity and/or frequency the absorption excitonic peaks show up near the band gap.

II. OPTICAL ABSORPTION UNDER TERAHERTZ RADIATION

Considering the QW driven both by a growth-direction-polarized electric field and an optical pulse as schematically shown in the inset of Fig. 1, the electric field expressed by

$$\mathbf{F}(t) = \mathbf{F}_{dc} + \mathbf{F}_{ac} \cos(2\pi f_{ac}t), \tag{1}$$

in which $\mathbf{F}_{dc}$ is the dc field, $\mathbf{F}_{ac}$ and f_{ac} are, respectively, the strength and the frequency of the THz field. For optical field, we introduce a real optical field $E(t) = (1/2)[F_{opt}(t) \times \exp(-i\omega_g t) + \text{c.c.}]$. The complex slowly varying envelope $F_{opt}(t)$ of the real optical field is assumed to be a Gaussian pulse as follows:

$$\mathbf{F}_{opt}(t) = \mathbf{F}_0 \exp[-t^2/\tau^2 - i(\omega_c - \omega_g)t] \tag{2}$$

in which τ is the temporal width of the pulse, ω_c is the central frequency, and ω_g is the band gap frequency. The QW driven by an electric field and an optical pulse can be described by the density matrix theory including both Coulomb and THz field induced intersubband couplings.[16–18] The Hamiltonian takes the form

$$H = H_0 + H_T + H_I + H_C, \tag{3}$$

where H_0 is the Hamiltonian of the QW in the absence of Coulomb interactions, the terahertz field, and the external optical field

$$H_0 = \sum_{\ell, \mathbf{k}} (\varepsilon_{e\mathbf{k}}^\ell a_\mathbf{k}^{\ell+} a_\mathbf{k}^\ell + \varepsilon_{h\mathbf{k}}^\ell b_\mathbf{k}^{\ell+} b_\mathbf{k}^\ell). \tag{4}$$

Here $a_\mathbf{k}^\ell(b_\mathbf{k}^\ell)$ and $a_\mathbf{k}^{\ell\dagger}(b_\mathbf{k}^{\ell\dagger})$ are the annihilation and creation operators for an electron (hole) with wave number $\mathbf{k}$ in ℓth subband. H_T stands for the interactions of the QW with the terahertz field $\mathbf{F}(t)$. It reads

---

[a)]Author to whom correspondence should be addressed; electronic mail: jccao@mail.sim.ac.cn
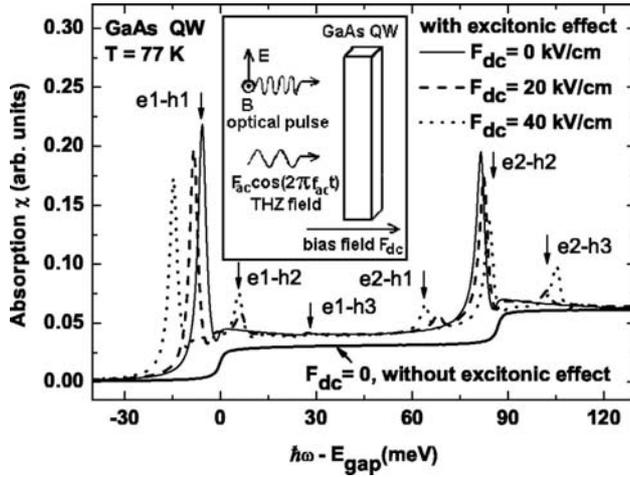
FIG. 1. Optical absorption including excitonic effects in quantum wells at different dc biases: $F_{dc}=0$, 20, and, 50 kV/cm, respectively. The step-like solid line shows the free-carrier optical absorption of unbiased quantum wells, excluding the Coulomb interaction. The inset shows a QW driven by a THz field and an optical field.

$$H_T = \mathbf{F}(t) \cdot \sum_{\ell,m,\mathbf{k}} \mu^{\ell m}(a_{\mathbf{k}}^{\ell +} a_{\mathbf{k}}^{m} - b_{\mathbf{k}}^{m+} b_{\mathbf{k}}^{\ell}), \qquad (5)$$

where μ is the intraband dipole matrix element.

H_I includes the interaction of QW with the optical pulse field given by

$$H_I = -|e|\mathbf{F}_{opt}(t) \cdot \sum_{\ell,m,k} (\mathbf{d}_{cv}^{\ell m} a_{\mathbf{k}}^{\ell +} b_{-\mathbf{k}}^{\ell +} + H.c.), \qquad (6)$$

where e is the carrier charge, $H.c.$ denotes the Hermitian conjugate of the first term. In the effective-mass approximation, we have

$$d_{cv}^{\ell m} = -e \int dr u_e(r)^* x u_h(r) \int dz \varphi_e^{\ell}(z) \varphi_h^{m}(z) \qquad (7)$$

in which $\int dr u_e(r)^* e x u_h(r) = 7/\sqrt{2}e$ Å $\simeq 4.9e$ Å when the conduction-band bulk Bloch state is assumed to be s-like, and the valence-band bulk state is p-like.

The electron-hole interaction term H_C is given by

$$H_C = \frac{1}{2} \sum_{m,\ell,p,s,\mathbf{q}} V_{\ell s}^{mp}(q) a_{\mathbf{k}-\mathbf{q}}^{p+} b_{\mathbf{k}'+\mathbf{q}}^{m+} b_{\mathbf{k}'}^{\ell} a_{\mathbf{k}}^{s}. \qquad (8)$$

Using the rotating-wave approximation relative to the band gap, the equation of the motion is obtained directly from the Hamiltonian

$$\hbar \frac{dp_{\mathbf{k}}^{m\ell}(t)}{dt} = -i(\varepsilon_{e\mathbf{k}}^{\ell} + \varepsilon_{h\mathbf{k}}^{m} - \hbar\omega_g)p_{\mathbf{k}}^{m\ell}(t) + i(n_{e\mathbf{k}}(t)$$
$$+ n_{h\mathbf{k}}(t) - 1)\omega_{R,\mathbf{k}}(t) + i\mathbf{F}(t)$$
$$\times \sum_n (\mu^{\ell m} p_{\mathbf{k}}^{mn} - \mu^{mn} p_{\mathbf{k}}^{n\ell}) - \Gamma_{sc} p_{\mathbf{k}}^{m\ell} \qquad (9)$$

in which $\hbar\omega_{R,k}(t) = \mathbf{d}_{cv} \cdot \mathbf{F}_{opt}(t)\delta_{\ell m} + \Sigma_{p,s,\mathbf{q}} V_{\ell s}^{mp}(\mathbf{k}-\mathbf{q})p_{\mathbf{q}}^{ps}$, $n_{e,\mathbf{k}} = \langle a_{\mathbf{k}}^{+} a_{\mathbf{k}} \rangle$, $n_{h,\mathbf{k}} = \langle b_{-\mathbf{k}}^{+} b_{-\mathbf{k}} \rangle$, $p_{\mathbf{k}}^{m\ell} = \langle b_{-\mathbf{k}}^{m} a_{\mathbf{k}}^{\ell} \rangle$, ω_g is the band gap frequency, and Γ_{sc} is the phenomenological dephasing term including the effects of electron-hole-phonon

and carrier–carrier (e-h, h-h) collisions. The time dependent carrier populations are determined by the semiconductor Block equation.[19] If we write $n_{\alpha,\mathbf{k}}(t) = n_{\alpha,\mathbf{k}}^{(0)} + \Delta n_{\alpha,\mathbf{k}}(t)$, the time-dependent part is determined by $\text{Im}[\omega_{R,k}(t)p_{\mathbf{k}}^{m\ell}(t)]$ and a collision term. The first term will contribute a high order term either in the optical field or in the polarization. The second term will contribute a higher order in carrier–carrier scattering. These high order contributions will be important in the large-q regime. The wave number of the THz and optical fields used in this work is still much shorter as compared to the Fermi wave vector. Therefore we only seek the linear response of the system to the optical pulse and neglect the time dependence of the carrier density. In Eq. (9) we use $n_{\alpha\mathbf{k}}^{(0)} = 1/[e^{\beta(\varepsilon_{\alpha\mathbf{k}} - \mu_\alpha)} + 1]$ for the electron/hole density, with α the carrier type (electron or hole), T is the lattice temperature, and μ_α is the carrier chemical potential determined by the carrier density

$$N = \frac{1}{A} \frac{1}{2\pi} \left(\frac{2mk_B T}{\hbar^2} \right) \int_0^\infty d\varepsilon_{\alpha k} \frac{1}{e^{[\varepsilon_{\alpha k} - \mu_\alpha]/k_B T} + 1}, \qquad (10)$$

in which A is the quantization area of the quantum well.

The slowly varying envelope polarization $P(t)$ of the real macroscopic optical polarization per unit area of the QW, $P(t)\exp(-i\omega_g t) + c.c.$, is related to the interband polarization matrix elements as follows:[20]

$$P(t) = \frac{d_{cv}}{A} \sum_{\mathbf{k},m,\ell} p_{\mathbf{k}}^{m\ell}(t). \qquad (11)$$

The optical absorption in the QWs is expressed by[20]

$$\chi(\omega) = \frac{4\pi\omega_g}{c\sqrt{\epsilon_b}} \frac{\text{Im}[P(\omega)E(\omega)^*]}{|E(\omega)|^2}, \qquad (12)$$

where $P(\omega)$ and $E(\omega)$ are the Fourier transforms of the polarization function $P(t)$ and of the laser pulse $\mathbf{F}_{opt}(t)$, respectively.

III. ABSORPTION IN THZ-DRIVEN GAAS QWS

We apply the above Eqs. (9)–(12) to perform the numerical calculations of the optical absorption spectra in GaAs QWs driven by the optical pulse and the THz field along the z axis, i.e, the growth direction of the QW. The GaAs QW has infinite barriers at $z = \pm L/2$ with L the QW width. The wave function for the confined carriers in the QW is expressed by the product of the bulk Bloch state $u_\alpha(r)$ and a slowly varying envelope, as follows:

$$\psi_{\alpha\mathbf{k}}^n(r) = u_\alpha(r)\varphi_\alpha^n(z)\frac{e^{ik \cdot r}}{\sqrt{A}},$$

where n is the subband index, $\mathbf{k}$ is the two-dimensional in-plane momentum, and $\varphi_\alpha^n(z)$ is the single-particle envelope function. We use the envelope functions at the unbiased case: $\varphi_\alpha^n(z) = \sqrt{2/L} \cos(n\pi z/L)$ when n is odd, and $\varphi_\alpha^n(z) = \sqrt{2/L} \sin(n\pi z/L)$ when n is even. The bound state energies are $\varepsilon_\alpha^\ell = \hbar^2 \pi^2 \ell^2/(2L^2 m_{e(h)\perp})$. The energy dispersion relation is $\varepsilon_{\alpha\mathbf{k}}^\ell = \varepsilon_\alpha^\ell + \hbar^2 \mathbf{k}^2/(2m_{\alpha\parallel})$. We consider two conduction subbands and three valence subbands. The material parameters used here are typical values of GaAs QWs: $m_{h\parallel}$

$=0.109m_0$, $m_{h\perp}=0.408m_0$, and $m_{e\parallel}=m_{e\perp}=0.067m_0$ with m_0 the free electron mass. The coupled first order differential equations [Eq. (9)] are solved using a fifth order Runge–Kutta algorithm. We have used the following boundary conditions: (i) in the remote past the conduction (valence) subbands are occupied; (ii) the polarizations are assumed to vanish in the remote past. The polarizations are solved from just before the optical pulse arrives to a final time when the interband polarization has essentially completely dephased (t is about 12 ps).

In this article, we are interested in the optical absorption near the band gap, so we set the Gaussian central frequency ω_c in Eq. (2) to be ω_g. Γ_{sc} is set to be 100 fs.[21] The temporal pulse width τ is assumed to be 20 fs and the power density of the optical pulse is assumed to be 50 W/cm^2. The total density is $N=1.2\times10^{11}$ cm^{-2}, the QW width is $L=15$ nm, and the lattice temperature is set to be throughout the paper $T=77$ K. In the calculation, we neglect the heating effect on the optical absorption.

Figure 1 shows the optical absorption $\chi(\omega)$ of the QW only driven by the dc fields. The lowest solid line is for the free-carrier optical absorption without the dc bias and the Coulomb interaction. There are two absorption steps which correspond to the $e1$-$h1$ and $e2$-$h2$ transitions. The positions of the $e1$-$h1$ and $e2$-$h2$ locate at the band gap and 88 meV above the band gap, respectively. When including the Coulomb interaction, the excitonic peaks show up instead of the steps observed in the absence of e-h interaction. Optical absorption including excitonic effects in quantum wells at different dc biases is: $\mathbf{F}_{dc}=0$, 20, and, 50 kV/cm, respectively, shown in Fig. 1. The position of the absorption peak coincides with those of the free-carrier absorption. The amplitudes of the transitions including the excitonic effect enhance slightly due to Coulomb coupling term, which are in agreement with the results reported.[10,22] When $F_{dc}=20$ and 40 kV/cm, it can be seen from Fig. 1 that there are four replicas besides the two main absorption peaks. These additional optical absorption peaks correspond, respectively, to $e1$-$h2$, $e1$-$h3$, $e2$-$h1$, and $e2$-$h3$ transitions. In the calculations, we neglect the electron–electron and hole–hole interactions, so the locations of the absorption peaks of the $e2$-$h1$, $e2$-$h2$, and $e2$-$h3$ transitions are slightly away from the transition energies. The strength of absorption peaks due to the $e1$-$h1$ and $e2$-$h2$ transitions becomes weak and the left absorption peak redshifts with increasing dc strength. However, the absorption peaks due to the $e2$-$h2$ and $e2$-$h3$ transitions blueshift with increasing dc strength.

Figure 2 shows the optical absorption of the QW driven by the terahertz fields. The frequency is 0.7 THz, and the THz strengths are 5, 20, and 40 kV/cm, respectively. It can be seen from Fig. 2 that the THz field induces a redshift in the absorption peak near the band gap. The THz radiation also causes a reduction in the magnitude of the absorption and the appearance of additional absorption peaks. Two replicas show up between the two main excitonic peaks, which correspond to the $e1$-$h1$ and $e2$-$h2$ transitions. It is indicated that the optical absorption is more sensitive to the presence of the THz field.

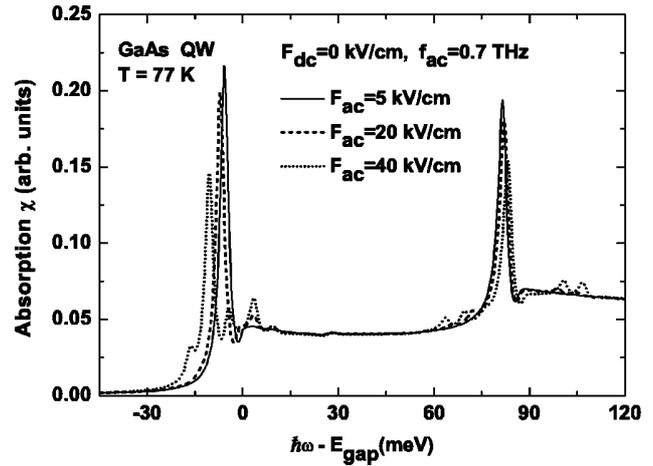Richer optical absorption spectra show up when the QW

FIG. 2. Optical absorption including excitonic effects at $F_{dc}=0$ kV/cm, $f_{ac}=0.7$ THz. The THz amplitudes are, respectively, $F_{ac}=5$, 20, and 40 kV/cm.

is driven both by the dc field and the THz field. In Fig. 3 we show the absorption spectra of the QW at $F_{dc}=40$ kV/cm, $f_{ac}=0.7$ THz, for several different ac amplitudes $F_{ac}=5$, 10, and 20 kV/cm. It can be seen that there is only one $e1$-$h1$ excitonic peak near the band gap when the THz strength is 5 kV/cm. When the THz strength increases to 10 kV/cm, the $e1$-$h1$ excitonic peak near the band gap splits into two peaks. This Autler–Townes splitting is due to the THz nonlinear dynamics of confined excitons and the sideband generation.[4] At the weaker ac fields, the splitting is so small that the two peaks form one broadened peak. When the THz strength increases to 20 kV/cm, the splitting is more noticeable and two replicas can been clearly seen. This is in agreement with the result of a recent experiment.[15] It is noted that the change of the strength of the THz field has little effect on the absorption peak due to the $e2$-$h2$ transition. The reason is that the energy of the $h1$-$h2$ transition is much greater than the frequency of THz field F_{ac} (0.7 THz$\approx$3 meV), thus does not resonate with the THz field. The absorption spectra of the QW at different THz frequencies is shown in Fig. 4.
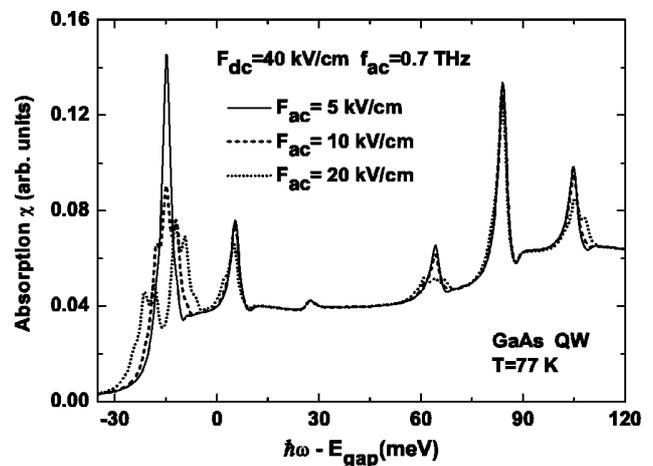

FIG. 3. Optical absorption including excitonic effects at $F_{dc}=40$ kV/cm, $f_{ac}=0.7$ THz. The THz amplitudes are, respectively, $F_{ac}=5$, 10, 20 kV/cm.
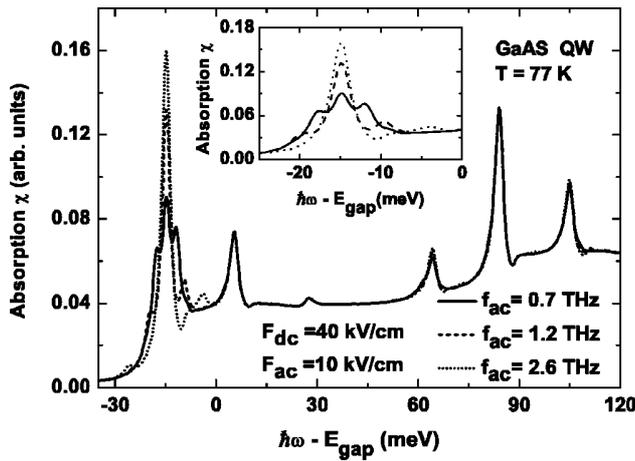
FIG. 4. Optical absorption including excitonic effects at $F_{dc} = 40$ kV/cm, $F_{ac} = 10$ kV/cm. The THz frequencies are, respectively, $f_{ac} = 0.7$, 1.2 and 2.6 THz.
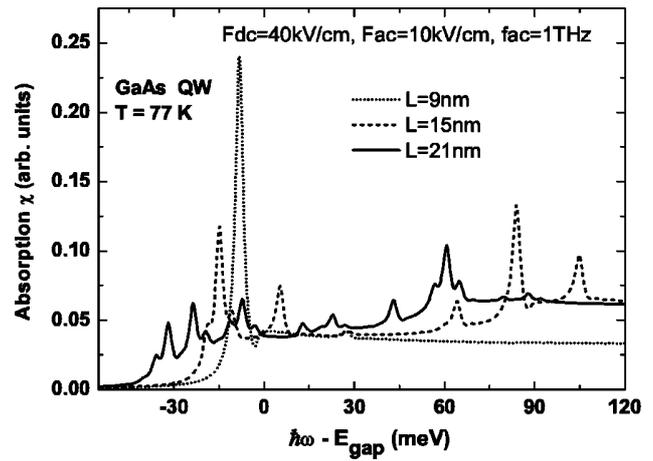

FIG. 6. Optical absorption including excitonic effects in quantum wells at $F_{dc} = 0$ kV/cm, $F_{ac} = 10$ and $f_{ac} = 1$ THz. The QW widths are $L = 9$, 15, and 21 nm, respectively.

The strength of dc field is fixed at $F_{ac} = 10$ kV/cm and the frequencies of THz field are 0.7, 1.2, and 2.6 THz, respectively. When $f_{ac} = 0.7$ THz, the amplitude of the center peak near the band gap is not much higher than that of the two replicas, shown in the inset figure in Fig. 4. With increasing of the THz frequency, the center peak becomes higher and the replica moves away from the center peak. The presence of these strong replicas indicates that there is the possibility of producing sidebands.[23]

To have an insight into the effect of the quantum well width on the transitions, we studied the optical absorption of the QW with different widths: $\ell = 9$, 15, and 21 nm. Figure 5 shows the optical absorption of the QW driven by dc field with the dc strength $F_{dc} = 30$ kV/cm. Many additional absorption channels open up as QW width increases. The reason is that with increasing the QW width, the energy between those subbands decreases which leads to more absorption peaks. Moreover, we can see from Fig. 5 that the amplitude of the exciton peak slightly decreases, and the absorption edge redshifts with increasing the quantum well width. When
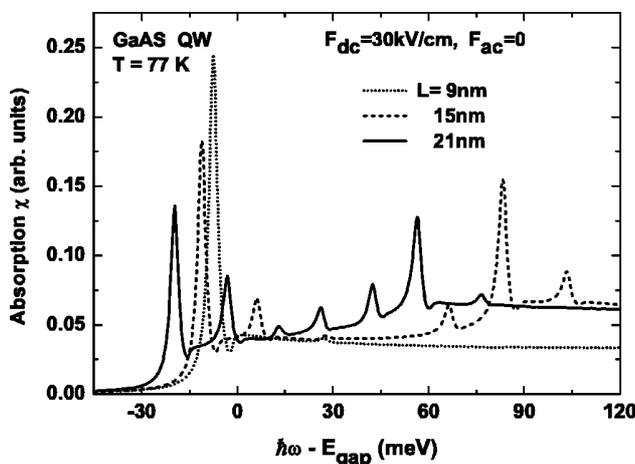
we apply the THz field to the quantum well, there are many replicas around those excitonic peaks, shown in Fig. 6. These are different from those shown in Fig. 5. The reason is that the coupling between the THz field and the subband becomes stronger as the subband energy gaps decrease. The dependence of the absorption spectra on the carrier density is shown in Fig. 7. The carrier densities are 1.2×10^{11}, 6.0×10^{11}, and 1.2×10^{12} cm^{-2}, respectively. We can see from Fig. 7 that the excitonic peak strengths decrease rapidly with increasing the carrier densities. Meanwhile, the spectral location of the excitonic peaks moves away slightly from the original locations. It means that an increased doping density can suppress the optical absorption. This density dependence of the optical absorption is mainly due to increased screening at large densities. The inter-band polarization increases with the screened inter-band interaction matrices. As density increases, the screening also increases and, as a result, the absorption decreases. It should also be noticed that we only used electron density in our calculation to determine the
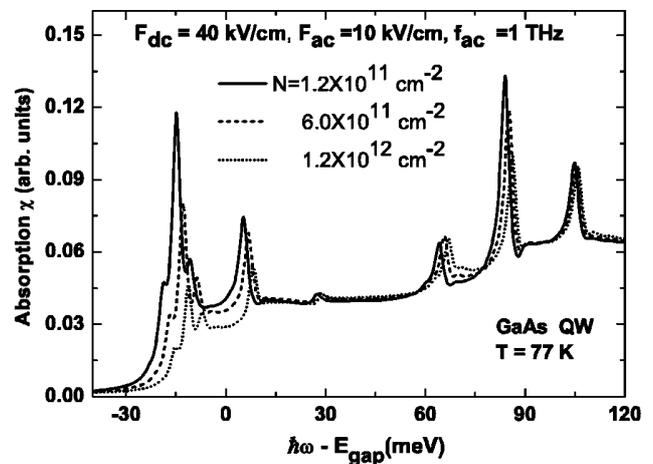

FIG. 5. Optical absorption including excitonic effects in unbiased quantum wells with the QW widths are $L = 9$, 15, and 21 nm, respectively.

FIG. 7. Optical absorption including excitonic effects in quantum wells at $F_{dc} = 0$ kV/cm, $F_{ac} = 10$ kV/cm and $f_{ac} = 1$ THz. The total carrier densities of QW are $N = 1.2 \times 10^{11}$, 6.0×10^{11}, and 1.2×10^{12} cm^{-2}, respectively.

chemical potential and screening length. Our system is an *n*-type quantum well. The hole density (mainly of photoexcited holes) is negligible as compared to the electron density. Our formalism can be readily extended to include both electron and hole densities. For samples with a comparable number of electrons and holes, both carriers will contribute to the screening and chemical potential dynamically adjusted due to varying electron and hole densities.

IV. CONCLUSION

In conclusion, we have studied the optical absorption spectra in doped GaAs QW driven by both the THz field and the optical pulse. We have obtained the detailed information of the optical absorption in a QW under an intense terahertz radiation. The dependence of the optical absorption on the intensity and frequency of the THz field, on the QW width and carrier density are studied. The calculated Autler–Towns splitting is in good agreement with the experiments.

ACKNOWLEDGMENTS

[1] A. V. Maslov and D. S. Citrin, Phys. Rev. B **64**, 155309 (2001).
[2] D. S. Citrin, Appl. Phys. Lett. **76**, 3176 (2000).
[3] A. V. Maslov and D. S. Citrin, IEEE J. Sel. Top. Quantum Electron. **8**, 457 (2002).
[4] J. Kono, M. Y. Su, T. Inoshita, T. Noda, M. S. Sherwin, S. J. Allen, and H. Sakaki, Phys. Rev. Lett. **79**, 1758 (1997).
[5] J. Černe, J. Kono, T. Inoshita, M. Sherwin, M. Sundaram, and A. C. Gossard, Appl. Phys. Lett. **70**, 3543 (1997).
[6] S. Hughes and D. S. Citrin, Phys. Rev. B **59**, R5288 (1999).
[7] K. B. Nordstrom, K. Johnsen, S. J. Allen, A. Jauho, B. Birnir, J. Kono, T. Noda, H. Akiyama, and H. Sakaki, Phys. Rev. Lett. **81**, 457 (1998).
[8] J. C. Cao and X. L. Lei, Phys. Rev. B **67**, 085309 (2003).
[9] J. N. Heyman, K. Craig, B. Galdrikian, M. S. Sherwin, K. Campman, P. F. Hopkins, S. Fafard, and A. C. Gossard, Phys. Rev. Lett. **72**, 2183 (1994).
[10] Y. Yacoby, Phys. Rev. **169**, 610 (1968).
[11] A. P. Jauho and K. Johnsen, Phys. Rev. Lett. **76**, 4576 (1996).
[12] T. Fromherz, Phys. Rev. B **56**, 4772 (1997).
[13] S. M. Sadeghi, J. F. Young, and J. Meyer, Phys. Rev. B **56**, R15557 (1997).
[14] A. Liu and C.-Z. Ning, J. Opt. Soc. Am. B **17**, 433 (2000).
[15] C. Phillips, M. Y. Su, M. S. Sherwin, J. Ko, and L. Coldren, Appl. Phys. Lett. **75**, 2728 (1999).
[16] H. Haug and A.-P. Jauho, *Quantum Kinetics in Transport and Optics of Semiconductors*, Springer Series in Solid-State Sciences Vol. 123 (Springer, Berlin, 1996).
[17] T. Kuhn, in *Theory of Transport Properties of Semiconductor Nanostructures*, edited by E. Schöll (Chapman and Hall, London, 1998), Chap. 10.
[18] E. Binder, T. Kuhn, and G. Mahler, Phys. Rev. B **50**, 18319 (1994).
[19] H. Haug and S. W. Koch, *Quantum Theory of the Optical and Electronic Properties of Semiconductors*, 3rd ed. (World Scientific, Singapore, 1994).
[20] A. V. Maslov and D. S. Citrin, Phys. Rev. B **62**, 16686 (2000).
[21] A. V. Kuznetsov, G. D. Sanders, and C. J. Stanton, Phys. Rev. B **52**, 12045 (1995).
[22] J. Hader, J. V. Moloney, and S. W. Koch, IEEE J. Quantum Electron. **35**, 1878 (1999).
[23] D. Sullivan and D. S. Citrin, J. Appl. Phys. **89**, 3841 (2001).